This is a preprint of: "Quadratic vector fields in class I", Joan Carles Artés, Hebai Chen, Lluc Manel Ferrer, Man Jia, *Dyn. Syst.*, vol. 40(2), 191–222, 2024.
DOI: [10.1080/14689367.2024.2436223]

QUADRATIC VECTOR FIELDS IN CLASS I

JOAN CARLES ARTÉS[1], HEBAI CHEN[2], LLUC MANEL FERRER[1] AND MAN JIA[2]

Abstract. Planar quadratic differential systems occur in many areas of applied mathematics. Although more than one thousand papers have been written on these systems, a complete understanding of this class is still missing. Classical problems, and in particular, Hilbert's 16th problem [28, 29], are still open for this class. Among many interesting families of quadratic systems, the ones which may have limit cycles are of specially interest. In [42], these systems where classified in three different normal forms (I, II and III) with increasing number of parameters. The simplest family is I and even several subfamilies of it have been studied, and some global attempts have been done, up to this paper, the full study was still undone.

In this article we make an interdisciplinary global study of the class I. Since the family has 4 parameters, we have studied it using the same technique that has already been used in several papers with similar systems which is based in the algebraic invariants of the Sibirskii's school.

The bifurcation diagram for this class, done in the adequate parameter space which is the 3–dimensional real projective space, is quite rich in its complexity and yields 261 subsets with 49 different phase portraits for Class I (two of them corresponding to linear systems), seven of which have limit cycles. The phase portraits are always represented in the Poincaré disc. The bifurcation set is formed by an algebraic set of bifurcations of singularities, finite or infinite and by an analytic set of curves corresponding to phase portraits which have separatrix connections.

Algebraic invariants were needed to construct the algebraic part of the bifurcation set, symbolic computations to deal with some quite complex invariants and numerical calculations to determine the position of the analytic bifurcation set of connections.

1. Introduction, brief review of the literature and statement of results

It is easy to find that there are many papers and monographs about many special classes quadratic vector fields, such as [1, 2, 3, 4, 5, 6, 7, 8, 9, 10, 11, 12, 13, 15, 16, 17, 20, 22, 24, 25, 31, 33, 36, 37, 38, 39, 43, 44, 45] and the references therein, in which limit cycles and global phase portraits in the Poincaré disc of many families of quadratic vector fields have been studied. One main reason is that many mathematicians have been highly interested in Hilbert's 16th problem since 1900. However, the problem is still intractable, see [30, 34], even for general quadratic vector fields. Fortunately, we have found that many classes quadratic vector fields were studied. For example, Artés et al. in [2] studied the structurally stable global phase portraits in the Poincaré disc of general quadratic vector fields, Artés et al. in [4] studied the structurally unstable global phase portraits in the Poincaré disc of general quadratic vector fields, Artés et al. in [6] studied the family of quadratic systems with a weak focus of second order, Reyn in [36] gave all global phase portraits in the Poincaré disc of quadratic systems without finite equilibria and in [37] studied quadratic systems with three finite singularites collided at infinity.

By [42], when a quadratic system exhibits a closed orbit, a necessary condition is that the quadratic system can be changed into one of the following three classes[1]:

$$\text{Class } I: \begin{cases} \dot{x} = y, \\ \dot{y} = -x + fy + \ell x^2 + 2mxy + ny^2, \end{cases} \tag{1}$$

2010 *Mathematics Subject Classification.* *Primary:* 34C40, 34C60, *Secondary:* 14D05.

Key words and phrases. Quadratic vector fields, phase portraits, bifurcation diagram.

[1]Ye in [42] used different parameter letters than here and did not put the "2" in the "xy" terms. We are using this notation since we are going to use invariant theory and this suits better with the system written in tensor form (see [14]).

where $(f,\ell,m,n)\in\mathbb{R}^4$;

$$\text{Class } II: \begin{cases} \dot{x}=y(1+2hx),\\ \dot{y}=-x+fy+\ell x^2+2mxy+ny^2, \end{cases} \tag{2}$$

where $(f,\ell,m,n)\in\mathbb{R}^4$ and $h\neq 0$;

$$\text{Class } III: \begin{cases} \dot{x}=y(1+2hx+ky),\\ \dot{y}=-x+fy+\ell x^2+2mxy+ny^2, \end{cases} \tag{3}$$

where $(f,h,\ell,m,n)\in\mathbb{R}^5$ and $k\neq 0$. When $\ell=n=0$ and $m\neq 0$, all global phase portraits in the Poincaré disc of system (1) were given in [32]. When $n=0$ and $\ell m\neq 0$, system (1) is a Bogdanov-Takens system. The uniqueness of limit cycles of the Bogdanov-Takens system was proven by Coppel in [21], and the bifurcation diagram and all global phase portraits in the Poincaré disc of the Bogdanov-Takens system were obtained by Perko in [35], where the number of topologically different global phase portraits in the Poincaré disc is 8. Gasull *et al* in [26] proved the Perko's conjectures in [35] about some analytic properties of the homoclinic bifurcation curve. Recently, Jia *et al.* in [31] completely gave the bifurcation diagram and all global phase portraits in the Poincaré disc of system (1) when $m=0$ and $n\neq 0$, where the number of global phase portraits in the Poincaré disc is 19. Notice that the dynamics of system (1) is very simple since the divergence of system (1) is f for $m=n=0$. This explains why the authors required $n\neq 0$ when $m=0$ in [31]. It is predictable that the bifurcation diagram and all global phase portraits in the Poincaré disc of system (1) for $\ell mn\neq 0$ are more complex than the previous two cases. Rychkov in [40] proved that system (1) exhibits at most one limit cycle, also refer to [42, 44]. Moreover, when $f=0$ and $m=1$, seven global phase portraits in the Poincaré disc are given in [42, pp. 269-270]. And Coll in his Ph. D. thesis [19] tried a global attempt on the whole family but some portraits were missing as we will show here. However, there are only some partial results for systems (2) and (3), such as [42, 43]. In other words, the maximum number of limit cycles of systems (2) and (3), i.e., quadratic vector fields in Classes II and III, are still unsolved.

Gouveia et al. in [27] classified the global phase portraits in the Poincaré disc of the quadratic polynomial Liénard systems

$$\begin{cases} \dot{x}=y,\\ \dot{y}=(ax+b)y+cx^2+dx+e, \end{cases} \tag{4}$$

where a,b,c,d,e are real parameters. When $ac\neq 0$, it is to note that system (4) is also a Bogdanov-Takens system. It is clear that most results of this manuscript are not included in [27], such as the bifurcation diagram and some phase portraits in the Poincaré disc.

In this paper we will completely classify all phase portraits of Class I and our main result is:

Theorem 1. *There exist 49 topologically distinct phase portraits for the quadratic vector fields of Class I. All these phase portraits are shown in Figure 1 (except the linear center that we take it apart from the classification). The 4-dimensional parameter space is divided in 261 regions,* 52 *of them are 3-dimensional,* 111 *are 2-dimensional,* 78 *are 1-dimensional and* 20 *are 0-dimensional. Moreover the following facts hold.*

- *There are 7 phase portraits with one limit cycle. Concretely they are* V_5, V_6, V_{13}, V_{31}, $1S_5$, $5S_5$ *and* $9S_3$.
- *There are 12 phase portraits with exactly one graphic. Concretely they are* $7S_1$, $7S_2$, $7S_4$, $7S_5$, $1.7L_1$, $3.8L_1$, $3.8L_2$, $3.8L_3$, $4.7L_1$, $5.7L_1$, P_9 *and* P_{13}.
- *There are 6 phase portraits with exactly one set of an infinite number of graphics. Concretely they are* $9S_1$, $9S_3$, $9S_4$, $9S_6$, $1.9L_1$ *and* $4.9L_1$.
- *There are 2 phase portraits with exactly one set of an infinite number of graphics plus an isolated graphic. Concretely they are* $7.9L_1$ *and* P_{11}.
- *There is one phase portrait with one limit cycle and one set of an infinite number of graphics. This is* $9S_3$.

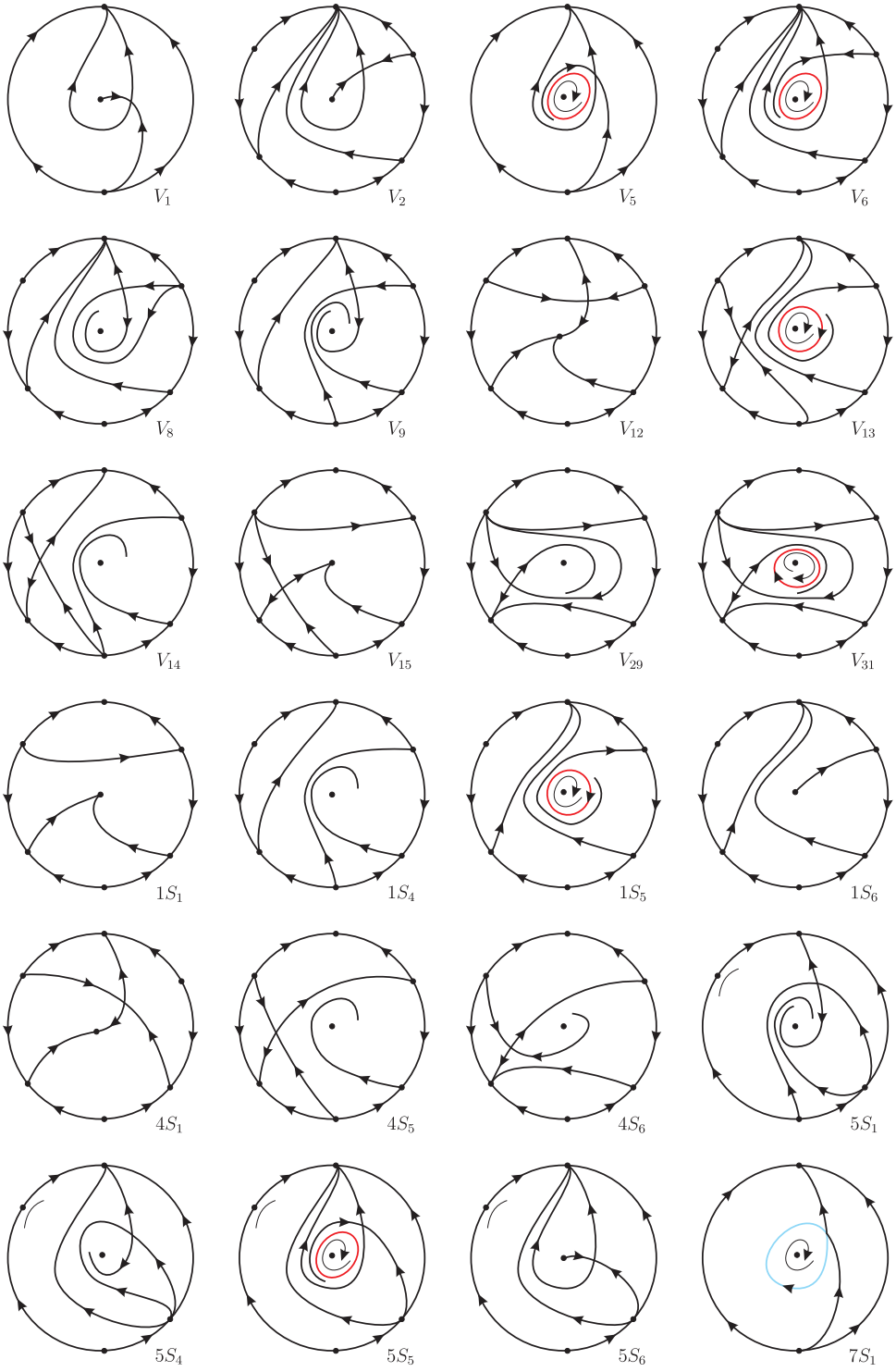

FIGURE 1. Phase portraits of the quadratic vector fields of Class I.

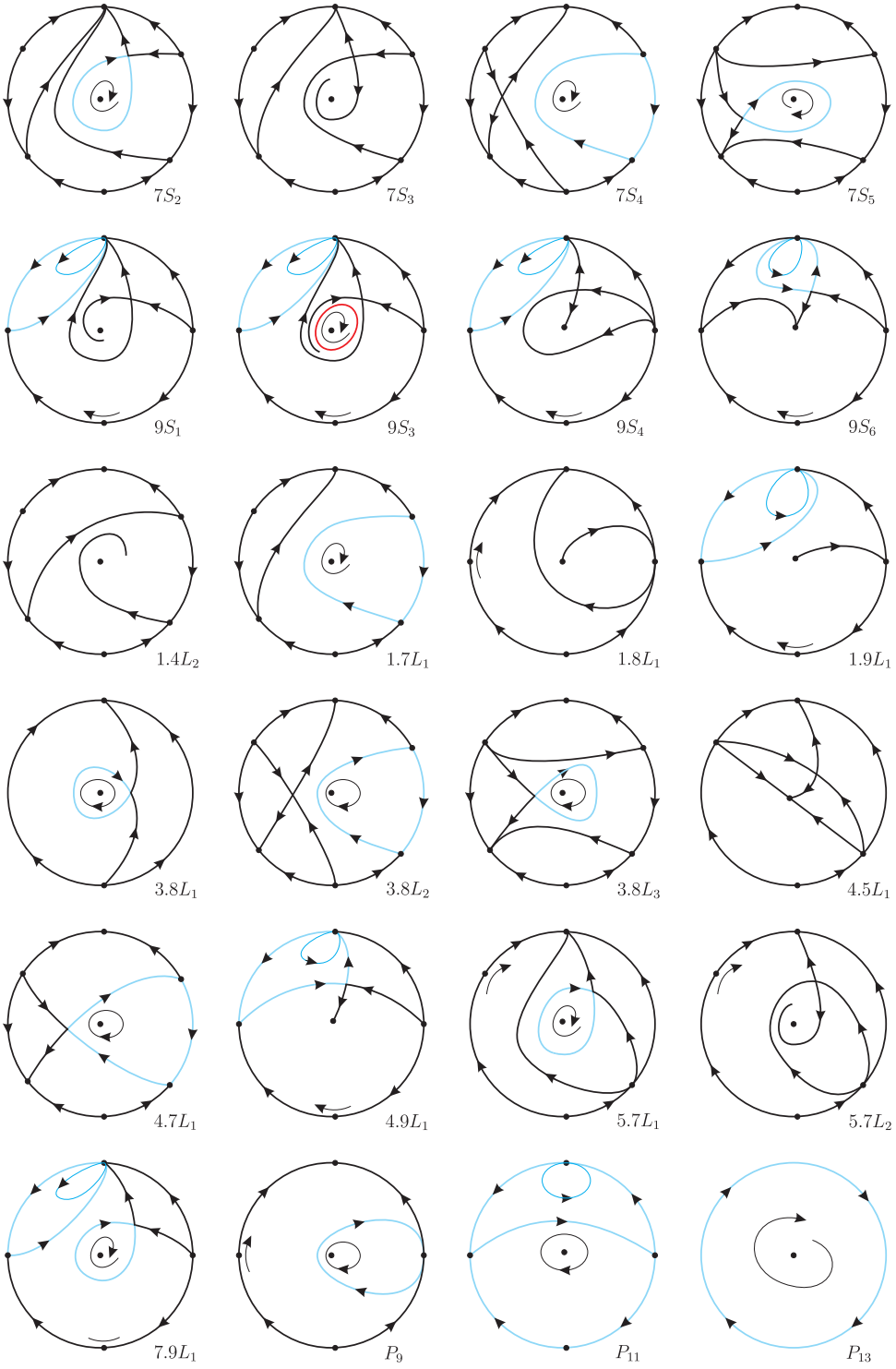

FIGURE 2. Continuation of Figure 1.

- *There are* 11 *phase portraits topologically equivalent to those shown in* [31] *and* 9 *from* [35].
- *The phase portraits* $4.5L_1$ *and* $4.7L_1$ *do not appear in the Ph. D. thesis of B. Coll* [19].

Remark 1. *It is worth to observe that even the family is 4-dimensional, all the topologically distinct phase portraits not contained in* [35] *and* [31] *(i.e. those with* $mn \neq 0$ *for which this paper is focused) may be found in a single 2-dimensional variety inside the parameter space. In fact any of the slices that we will present later produces all the new phase portraits. However it is not possible to prove this fact until the complete study is done, and some phase portraits with some geometrical features as invariant straight lines may be found only in some slices and not in others. This property somehow explains why Coll, in his Ph. D. thesis was so close to the complete classification even he only considered some parts of the bifurcation diagram.*

In Figure 1 we draw all the phase portraits in the Poincaré disc with separatrices in black wide colour. In some portraits we also add one or more orbits in black thin to better describe the behavior of the flow as for example in $5S_1$ to describe the flat hyperbolic sector at infinity, or $7S_1$ to describe the flow inside the graphic. We denote with a black dot all the singularities except the finite saddles which are already quite clear enough. We have drawn the graphics in blue color and the limit cycles in red color.

An outline of this paper is as follows. In Section 2, we prepare the parameter space so to reduce it in order to be easier to work with. In Section 3, we locate all the algebraic bifurcation surfaces using the invariants given by the Sibirskii School [14], divide the parameter space in two-dimensional slices and detect the most critical ones. In Section 4 we start by studying completely one main slice and there detect the existence of other non-algebraic bifurcation surfaces. After, we complete the other slices by checking the changes produced from neighbor ones. In Section 5 we complete the proof of Theorem 1 by extracting from all 'phase portraits found, those which are topologically different and indicating the groups of equivalent ones.

2. Preparing the parameter space

Systems (1) depend on the parameter $\lambda = (f, \ell, m, n) \in \mathbb{R}^4$. We will consider all systems (1) except the linear center, i.e. $\lambda = (f, \ell, m, n) \neq (0, 0, 0, 0)$. In this case a system (1) can be rescaled. We split the work in the cases $n \neq 0$ and $n = 0$. In the first case, the change $(x, y, t) \to (x/n, y/n, t)$ transforms system (1) into

$$\begin{aligned} \dot{x} &= y, \\ \dot{y} &= -x + fy + \ell/n x^2 + 2m/n xy + y^2, \end{aligned}$$

that is, with a renaming of variables $(\ell/n, m/n) \to (\ell, m)$, we may assume $n = 1$. Moreover the change $(x, y, t) \to (x, -y, -t)$ produces system

$$\begin{aligned} \dot{x} &= y, \\ \dot{y} &= -x - fy + \ell x^2 - 2mxy + y^2. \end{aligned}$$

So, we may consider only the semi-space $m \geq 0$. Finally we will divide the 3-dimensional space (f, ℓ, m) into slices so to study the whole space. The case $n = 0$ may be divided also in two cases $m \neq 0$ and $m = 0$. In a similar way, in the case $m \neq 0$ we will be able to assume $m = 1$ and we will have a two-dimensional space to study. And following the pattern, if $n = m = 0$ we may split it in $\ell \neq 0$ and $\ell = 0$. In the first case, we can also assume $\ell = 1$. In resume, we split a 4-dimensional space (minus one point) in the union of a set of 4 spaces of dimensions 3, 2, 1 and 0. In some other studies of the same kind (as for example [6]), where the parameters affected only the quadratic part of the equations, the authors were able to identify the 4-dimensional parameter space (minus one point) with the 3 dimensional projective space, which can be also seen as the ball $\mathbb{S}^3$ with identification of opposite points. In this ball, the case $n = 0$ (the surface of the ball) would correspond to the infinite "cover" of the affine 3-dimensional space, and the set $m = n = 0$ would correspond to the equator of the ball.

In our case, the presence of a parameter in the linear part of the equation does not allow the identification of our parameter space with the projective space since we will not have the equivalence between opposite points of the equator, but apart from that detail, the same technique used in [6] may be used here.

3. Study of the bifurcation diagram

At this point, classical works start by locating the singularities, finite and infinite of the normal form under study, their Jabobian matrices, determinants, traces and discriminants, and in case the singularities are not elementary, start applying the corresponding theorems which classify them, or start doing blow-ups. And if the singularities are linear centers, start computing Lyapunov constants in order to determine if they are centers surrounded by periodic orbits or weak foci of a certain order.

But the introduction of the algebraic invariants applied to polynomial differential systems (and more specifically quadratic systems) has meant a revolution in the study of Qualitative Theory. In previous years, it was needed that normal forms were simple enough so that singularities could be computed with no more than square roots, otherwise, all upcoming computations became too hard to follow. The algebraic invariants (used first in [6] and completed with the book [14]) allow to easily detect all the varieties which imply some bifurcation of the differential equation related with singularities. For every geometric feature that a singularity may have, there is one (or several) invariants which rule it. And these invariants can be computed for any normal form without need to compute the singularities. Also invariants to detect the existence of invariant straight lines have been found. Only non algebraic (or even non-analytic) features as some separatrix connections or double limit cycles cannot be detected by these algebraic invariants, but their presence is easily determined by means of coherence and continuity arguments, once the algebraic bifurcation diagram is completed.

3.1. **Algebraic surfaces.**

Bifurcation surface where a finite singularity coalesces with a singularity at infinity.

($\mathcal{S}_1$) For family (1) we already have that two finite singularities have coalesced with infinite singularities and this fact is recorded by the invariants $\mu_0 = \mu_1 = 0$. We also have always one singularity at the origin. So, the only possible bifurcation due to this phenomena is that a third finite singularity escapes to infinity, and this is captured by invariant μ_2 which for family (1) is simply the comitant

$$\mu_2 = \ell(\ell x^2 + 2mxy + ny^2)$$

when this comitant is zero for a non zero measure space in variables (x, y). In order to happen this, either $\ell = m = n = 0$ or simply $\ell = 0$. So, we will define surface

$$\mathcal{S}_1 : \ell = 0$$

and we will draw it in blue in the different bifurcation diagrams.

Bifurcation surface where the system has a weak finite singularity.

($\mathcal{S}_3$) Classicaly only weak foci were objects of interest in bifurcation diagrams since they are non-elementary singularities whose perturbation may produce limit cycles. And weak saddles appear rarely in bifurcation diagrams since their topological effect must be linked with the existence of a loop on that same saddle. However, by Vulpe's Theorem [14, Theorem 6.2] it is proved that weak saddles and weak foci are very close objects and the same invariants rule them both, even their degree of weakness. There is also other invariants (as $\mathcal{T}_3\mathcal{F}$) whose sign determines if the detected weak singularity is a saddle of a focus.

In our case, the invariant that detects the existence of one weak singularity is

$$\mathcal{T}_4 = 4f(f\ell + 2m)n(-m^2 + \ell n)$$

when this invariant is zero. So we will define surface

$$\mathcal{S}_3 : f(f\ell + 2m)n(-m^2 + \ell n) = 0$$

and we will draw it in solid yellow when it captures a weak focus and with dashed yellow when it captures a weak saddle (to reflect the topological relevance of the first in front of the second).

Bifurcation surface where at least two infinite singularities coalesce.

($\mathcal{S}_5$) The invariant that captures the coalescence of two infinite singularities is η which for family (1) is

$$\eta = 4n^2(m^2 - \ell n).$$

So we will define surface

$$\mathcal{S}_5 : n(m^2 - \ell n) = 0$$

and we will draw it in red.

Bifurcation surface where we have a focus-node transition.

($\mathcal{S}_6$) An elementary point whose discriminant of its jacobian is zero is a node but a small perturbation of it may turn it into a focus. This phenomena is captured by invariant W_4 which for family (1) is

$$W_4 = 16(-2 + f)(2 + f)(4\ell^2 + f^2\ell^2 + 4f\ell m + 4m^2)n^2(-m^2 + \ell n)^2.$$

So we will define surface

$$\mathcal{S}_6 : (-2 + f)(2 + f)(4\ell^2 + f^2\ell^2 + 4f\ell m + 4m^2)n(-m^2 + \ell n) = 0$$

and we will draw it in dashed black since it does never imply a topological change.

Existence of an invariant straight line.

($\mathcal{S}_4$) This bifurcation surface will contain the values of the parameters for which we possibly have an invariant straight line in the portrait. We note that this straight line will always exist unless it has gone to infinity. Therefore, the existence of an affine invariant straight line is not guaranteed on this surface. We note that this is a necessary but not sufficient situation. Notice also that the invariant line may coincide with a connection of separatrices in which case it is topologically relevant, or not. This invariant line feature is captured by the set of comitants B_1, B_2 and B_3. Since for family (1) the invariant B_1 is always zero, we must put our attention to comitant B_2 which is

$$\begin{aligned} B_2 = &-648(\ell^2 + 2f\ell m + 4m^2 - 2\ell n + f^2\ell n + 2fmn + n^2) \\ &(\ell^2 + 2f\ell m + 2\ell n + f^2\ell n + 2fmn + n^2)x^4. \end{aligned}$$

So we will define surface

$$\begin{aligned} \mathcal{S}_4 : &(\ell^2 + 2f\ell m + 4m^2 - 2\ell n + f^2\ell n + 2fmn + n^2) \\ &(\ell^2 + 2f\ell m + 2\ell n + f^2\ell n + 2fmn + n^2) = 0 \end{aligned}$$

and we will draw it in solid magenta when it corresponds with a separatrix connection and with dashed magenta when it does not.

Other surfaces.

($\mathcal{S}_9$) The case $n = 0$ and $m \neq 0$ (taken as $m = 1$) which will correspond to one full slice under study belongs both to surfaces $\mathcal{S}_3$ and $\mathcal{S}_5$. We call it with a different number to remind the double meaning it has. In this surface, the invariant $\mathcal{T}_4$ vanishes as well as $\mathcal{T}_3 = \mathcal{T}_2 = \mathcal{T}_1 = 0$ but $\sigma = f + 2mx^2 \neq 0$. So we are in condition (e) of [14, Theorem 6.2] and the next relevant invariant is $\mathcal{F}_1 = 2\ell m$. So, the role to decide the type of weak singularity is captured by the parameter ℓ. Thus, the straight line $\ell = 0$ will be denoted with code "3" as in $3.9L_1$ in this surface. Moreover, this slice coincides with the case already studied in [35].

($\mathcal{S}_8$) We will call surface $\mathcal{S}_8$ to the case $m = 0$ and $n \neq 0$ (taken as $n = 1$) which corresponds to one full slice under study. The value $m = 0$ does not vanish any needed invariant, but on this slice, several invariants coincide. Moreover, this slice coincides with the case already studied in [31].

The set $n = m = 0$ will be denoted as the line $8.9L$ (plus some points) and will play the role of the "equator" of the parameter space.

Finally, there exists another non-algebraic (and possible also non-analytical) surface where we will find separatrix connections. We will call such surface as $\mathcal{S}_7$ and we will draw it in solid magenta, the same as $\mathcal{S}_4$ since in both cases we have separatrix connections, but the name of the regions, whether they are $4S_i$ or $7S_i$ will indicate us the type of connection it is. This surface can only be detected by means of coherence arguments as we will do in Section 5.

Existence of an invariant parabola.

The algebraic invariants to detect an invariant conic have been recently developed by Vulpe et al. [41], but we will not use them here since they are quite many and heavy invariants, and we simply need to detect the presence of such a parabola in a few specific cases. In order that an invariant parabola may be relevant for our study, we need it to conform a separatrix connection and this implies that we must have an infinite singularity at least of nilpotent type. This implies that we must be on the surface $\mathcal{S}_5$. So, we will prove next lemma:

Lemma 1. *On every slice $m = m^*$ (thus $n = 1$), the point $(f, \ell, m) = (-m^*/2, (m^*)^2, m^*)$ produces a phase portrait with an invariant parabola. Moreover, one of the branches of the parabola corresponds to a separatrix connection between the finite saddle and an infinite saddle-node. The phase portrait obtained is $5.7L_2$ from Figure 1.*

Proof. We start from family of systems (1) which for $\ell = m^2/n$ (i.e. $\eta = 0$) have a double infinite singularity (in fact it is a multiplicity 4 singularity coming from the coalesence of two infinite and two finite singularities) at the point $[-m : n]$ of local chart U_1. We apply a rotation of angle $-\arctan(\frac{n}{m})$ so to move this infinite singularity at the point $[0 : 0]$ of local chart U_2 and we obtain the family of systems:

$$\begin{aligned}\dot{x} &= \frac{fx}{m^2+1} + \frac{y\left(fm + m^2 + 1\right)}{m^2+1} + \sqrt{m^2+1}\, x^2\\ \dot{y} &= -\frac{x\left(-fm + m^2 + 1\right)}{m^2+1} + \frac{fm^2 y}{m^2+1} + \sqrt{m^2+1}\, mx^2.\end{aligned}$$

Then, if this system has an invariant parabola passing through the point $[0 : 0]$ of local chart U_2 (or its symmetric), this parabola will have the form $F : y = a\,x^2 + b\,x + c$. And it is a simple exercise to check that the condition $f = -m/2$ is needed so to obtain the desired parabola with parameters

$$(a, b, c) = \left(-\frac{2\sqrt{m^2+1}\,\left(m^2+1\right)}{m^2+2}, -\frac{m^3}{m^2+2}, \frac{\sqrt{m^2+1}}{m^2+2}\right).$$

The existence of the separatrix connection comes from the fact that the parabola passes through the finite saddle at $(1/m^2, 0)$ (then it conforms its two stable separatrices), does not pass through any other finite singularity and that the singularity $[0 : 0]$ of local chart U_2 is a

nilpotent saddle-node. So the parabola arrives to this point on one side along one orbit of the parabolic sector, but on the other side it can only be the separatrix of the saddle-node. □

3.2. **Location of the singular slices.**

Since we our parameter space is $\mathbb{R}^4$ minus one point, and this can be identified with a union of spaces $\mathbb{R}^3 \cup \mathbb{R}^2 \cup \mathbb{R}^1 \cup \mathbb{R}^0$, most of the work will take place when studying the $\mathbb{R}^3$ part, and in it, we will split the parameter space in planes. We do not need to study an infinite number of planes. The bifurcation surfaces may have singularities and may intersect among them generically, so there will be slices whose partition due to the bifurcation surfaces will be topologically equivalent. But there will be some "singular" slices where either three (or more) surfaces will intersect, or the singular part of one surface intersects another surface, or other geometrical features which will make such slices special. We must detect all those singular slices. The next lemmas help us in such goal.

Lemma 2. *For $n = 1$ and $m = 1$, the surfaces $\mathcal{S}_3$, $\mathcal{S}_4$, $\mathcal{S}_5$ and $\mathcal{S}_6$ intersect them all at the point $f = -2$ and $\ell = 1$. Moreover the surfaces $\mathcal{S}_4$ and $\mathcal{S}_5$ are tangent at that point.*

Lemma 3. *For $n = 1$ and $m = 1/2$, the surfaces $\mathcal{S}_1$, $\mathcal{S}_4$ and $\mathcal{S}_6$ intersect each other in the point $f = -2$ and $\ell = 0$. Moreover the surfaces $\mathcal{S}_4$ and $\mathcal{S}_6$ are tangent at that point.*

Lemma 4. *For $n = 1$ and $m = 1/3$, the surfaces $\mathcal{S}_3$, $\mathcal{S}_4$ and $\mathcal{S}_6$ intersect each other at the point $f = 2$ and $\ell = -1/3$.*

Lemma 5. *For $n = 1$ and $m = 1/4$, the surfaces $\mathcal{S}_1$, $\mathcal{S}_4$ and $\mathcal{S}_6$ intersect each other at the point $f = -2$ and $\ell = 0$.*

Lemma 6. *For $n = 1$ and $m = 2$, the point $(f, \ell) = (-1, 4)$ at which we have the invariant parabola belongs to surface $\mathcal{S}_3$.*

Lemma 7. *For $n = 1$ and $m = 4$, the point $(f, \ell) = (-2, 16)$ at which we have the invariant parabola belongs to surface $\mathcal{S}_6$.*

All the surfaces (except $\mathcal{S}_4$) are very simple, and this allows that all these lemmas can be proved easily with basic algebra tools.

Our decision to split the 3-dimensional space in slices of the type $m = cte$ comes now to effect since we realize that the singular slices defined by the previous lemmas are precisely $m = 0$, $1/4$, $1/3$, $1/2$, 1, 2, 4. Between each couple of these slices, and about the topmost one, we will take another value for m to chose a generic slice. That is, since these are all the singular slices, the bifurcation diagram on any other slice will remain topologically the same for small changes in m meanwhile it remains in the same interval between singular slices. In other papers using this same technique, it was found that apart from the singular slices produced by the algebraic bifurcation surfaces, other singular slices were produced when the non algebraic surface $\mathcal{S}_7$ intersected some other surfaces. These other singular slices could only be determined by continuity arguments and their values only computed numerically by bisection, and just in a approximate way. However, in this paper, we have found two of these singular slices, and we have been able to give an algebraic value since they coincide with the cases where the separatrix connection takes form of a parabola, and thus we have obtained the values $m = 2$ and $m = 4$ when surface $\mathcal{S}_7$ intersects $\mathcal{S}_3$ and $\mathcal{S}_6$ respectively. It is not impossible that a non-algebraic surface may intersect another surface (or even show a singularity) on an algebraic variety.

The surface $\mathcal{S}_9$ ($n = 0$ and $m = 1$) may be viewed as the slice of $m = \infty$, and the coherence of the bifurcation diagram on it, and its phase portraits with those of the topmost slice we will take, will proof that the bifurcation diagram is complete without need of other slices. So, the

slices we will use will be:

$$\begin{array}{ll} m_0 = 0 & m_8 = 1 \\ m_1 = 1/8 & m_9 = 3/2 \\ m_2 = 1/4 & m_{10} = 2 \\ m_3 = 2/7 & m_{11} = 3 \\ m_4 = 1/3 & m_{12} = 4 \\ m_5 = 2/5 & m_{13} = 5 \\ m_6 = 1/2 & m_{14} = \infty \,(\text{i.e. } n = 0,\, m = 1). \\ m_7 = 2/3 & \end{array}$$

The even subindeces correspond to the singular slices and the odd ones to the generic ones.

The subsets of the partition of the parameter space of dimensions 3, 2, 1 and 0, will be denoted respectively by (V), (S), (L) and (P) for Volume, Surface, Line and Point, respectively. The surfaces are named using a number which corresponds to each bifurcation surface which is placed on the left side of S. To describe the portion of the surface we place an index. The curves that are intersection of surfaces are named by using their corresponding numbers on the left side of L, separated by a point. To describe the segment of the curve we place an index. Volumes and Points are simply indexed (since three or more surfaces may be involved in such an intersection). If three or more surfaces intersect not just in a point but along a Line, we will use the code of the two surfaces with stronger geometrical meaning.

We consider an example: the surface $\mathcal{S}_3$ splits into 16 different 2–dimensional parts named from $3S_1$ to $3S_{16}$, plus some 1–dimensional arcs named as $3.xL_y$ or $x.3L_y$ (where x denotes the other surface intersected by $\mathcal{S}_3$ and y is a number), and some 0–dimensional parts. Then, for example, in Figure 3 we may see **V1** (respectively **1S1**, **1.4L1**) which stands for V_1 (respectively $1S_1$, $1.4L_1$). And the same happens with many other pictures.

4. Study of the main slice

We start by taking one generic slice. Normally we chose either the topmost or the bottom most generic slice. However in this case we started by $m = m_9 = 3/2$ and[2] we put there, in their respective color, all its intersections with the algebraic surfaces already described. The image we show is not numerically exact since some parts of the bifurcation diagram would be too small to put there a label, or even sometimes almost invisible. So we produce a topologically equivalent image of the bifurcation diagram, respecting also the tangencies between surfaces (see Figure 3). Then we label every region on it: the two dimensional parts correspond in fact to Volumes in the 3-dimensional bifurcation diagram, and so on. Since this slice is generic, the parts which are seen as points and in fact lines in the bigger space. The reader may notice that we have skipped some labels as for example V_5, V_6, V_8 and others since we will need these labels later and we will explain it in short.

Then, knowing that inside every part, the number and type of the singularities is already known using the signs of invariants and the tables from [14], we use program P4 (see [23]), to obtain one phase portraits of every region. We check if the phase portraits of the 3-dimensional regions are coherent with those of the borders of the regions. If there is coherence, then there is no need of existence of another bifurcation related with separatrix connections, but if there is no such coherence, then this proves that such a bifurcation must split that region in two or more pieces. This is what happens for example in V_7 since the phase portrait we obtain for a point close to $3S_5$ is different from the one we obtain at a point close to $3S_4$, Concretely, the phase portrait close to $3S_4$ contains a limit cycle while the other not. This phenomena happens

[2]The history is that we were initially convinced that the slice $m = m_{10} = 2$ was generic and started there, but later we realized that it was singular for a very particular detail related with non-algebraic surface $\mathcal{S}_7$, and that even another singular slice ($m = m_{13} = 4$) was above. Since all the regions were already named and renaming most of them could lead to mistakes, we preferred to start with generic slice $m = m_9 = 3/2$.

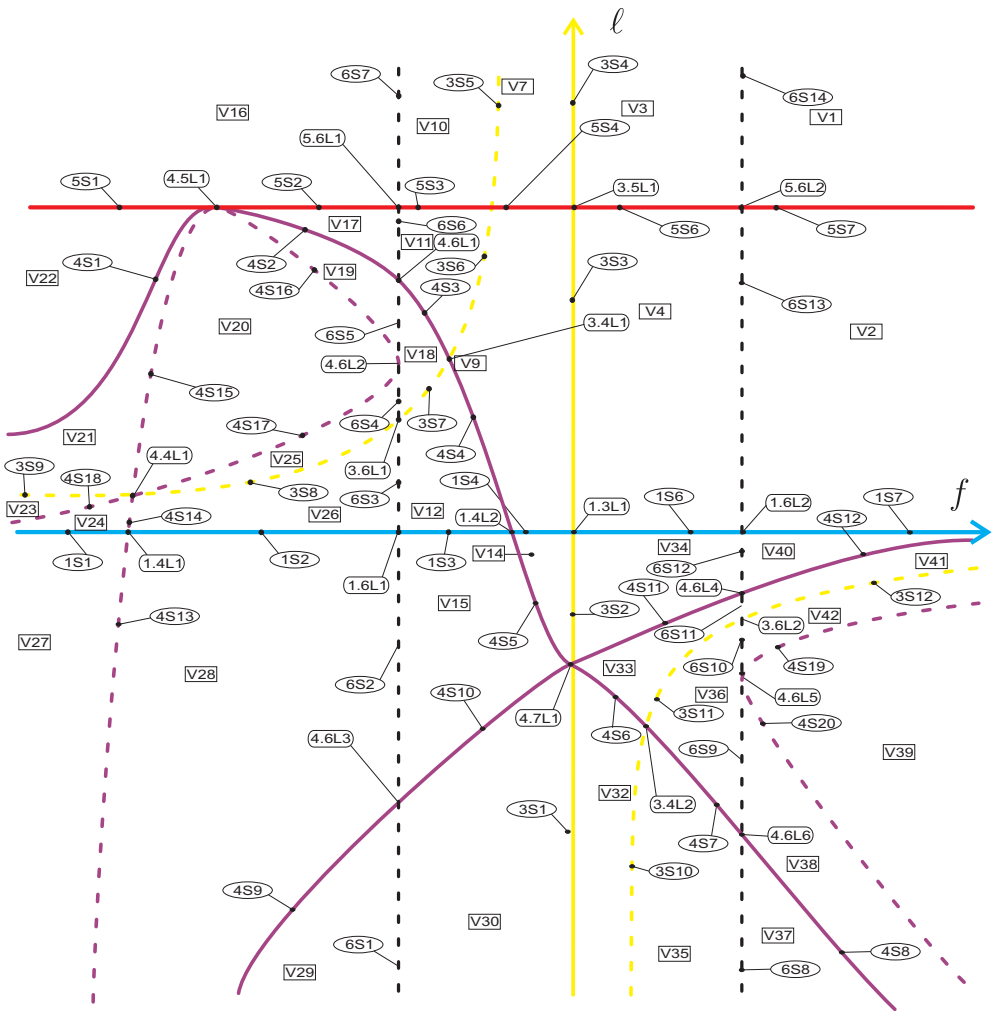

FIGURE 3. Bifurcation diagram for slice $m = m_9 = 3/2$ with only the algebraic bifurcation surfaces.

usually linked to the surface $\mathcal{S}_3$ when this surfaces detects the presence of a weak focus, which by the Poincar-Hopf bifurcation may produce one limit cycle close to it. The limit cycle that it is produced when we cross $3S_4$ coming from V_3 must disappear in some graphic which is not captured by any of the algebraic bifurcation surfaces we have detected. So, there must be a piece of surface $\mathcal{S}_7$ splitting region V_7 in two regions, which we rename as V_7 and V_5. In V_5 we have the limit cycle and in V_7 not. The part of $\mathcal{S}_7$ producing the bifurcation receives the name of $7S_1$ (see Figure 4) and portrays a loop where the limit cycle of V_5 dies. Even more, in region V_9 we have a similar phenomena since the bifurcation surface $\mathcal{S}_7$ prolongs its part $7S_1$ into $7S_2$ splitting regions V_6 from V_9. But this is not enough since the phase portrait V_8 that we obtain when the loop breaks, is not the same as the V_9 we obtain close to $3S_6$ or $4S_4$. So surface $\mathcal{S}_7$ needs to have another component where another separatrix connection not linked to a graphic must occur. This way we obtain phase portrait $7S_3$ which is the border between V_8 and V_9. The

prolongation of $7S_1$ into $7S_2$ induces a crossing point with surface $\mathcal{S}_5$ which is the line $5.7L_1$ splitting $5S_4$ from $5S_5$.

Notice that the parts $7S_1$ and $7S_2$ deal with the connection of separatrices of one same finite saddle forming a loop, and this has logical sense at both sides of surface $\mathcal{S}_5$. However, part $7S_3$ deals with the connection of a separatrix of a finite saddle with the separatrix of an infinite saddle. So, when we cross surface $\mathcal{S}_5$ and two infinite singularities become complex, such separatrix connection may not persist (at least in the real set) and the bifurcation must stop at $\mathcal{S}_5$. In principle, the part $7S_3$ could have ended on any point of surface $\mathcal{S}_7$, but the bifurcation values $m = m_{10} = 2$ and $m = m_{12} = 4$ detect when surface $\mathcal{S}_7$ intersects surfaces $\mathcal{S}_3$ and $\mathcal{S}_6$ respectively. So we have that for values $m < m_{10} = 2$, the part $7S_1$ ends at a point in surface $\mathcal{S}_5$ between $3.5L_1$ and $3.5L_2$ and since it must be right to the recently detected $5.7L_1$, it must split segment $5S_4$ in two subsegments renamed $5S_4$ and $5S_{10}$.

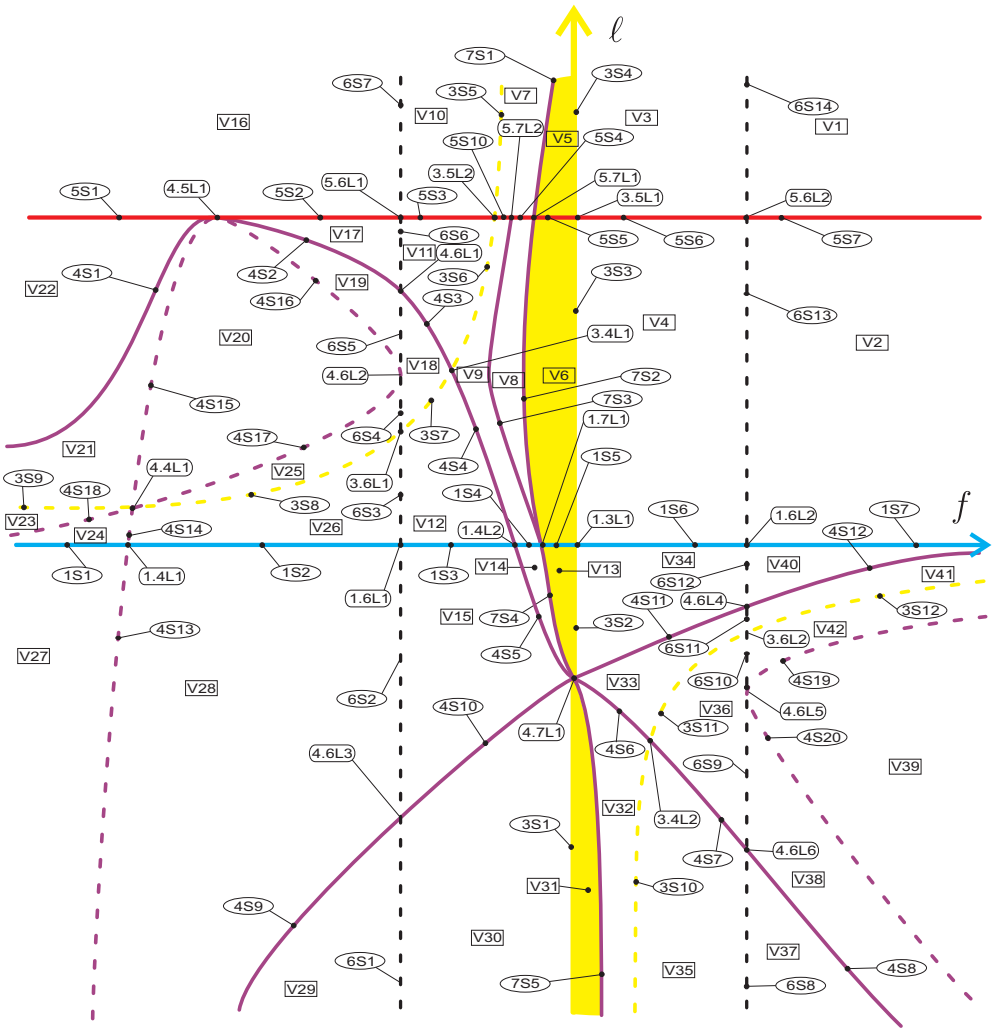

FIGURE 4. Bifurcation diagram for $m = 1.5$.

In a similar way, if we follow parts $7S_2$ and $7S_3$ down towards surface $\mathcal{S}_1$ (in blue) we see that the saddle that produces both connections is escaping towards infinity, and once it coalesces with an infinite singularity and the saddle remains at infinity, the loop connection is no more possible. So, below surface $\mathcal{S}_1$ only one part with separatrix connection may remain which is denoted by $7S_4$ needed also to split V_{13} with limit cycle from V_{14} without. Part $7S_4$ must end at $4.7L_1$ where we have a system with a center and reappears later as $7S_5$ needed to split V_{31} with limit cycle from V_{32} without.

Observation 1. *Notice that the parts $7S_1$ to $7S_5$, of the surface $\mathcal{S}_7$ could at some point cross the surface $\mathcal{S}_3$ which we have draw in dashed yellow because it corresponds to the weak saddle. But in case it happened, since the only finite saddle would be weak, that would imply that at some point, two limit cycles would be possible and this is in contradiction with Rychkov result* [40] *that states that systems* (1) *have at most one limit cycle. In principle it would be possible that $\mathcal{S}_7$ were tangent at some point with surface $\mathcal{S}_3$ but apart from its unstability, it would not create any new topologically different phase portrait, so we have not drawn any such contact.*

Now we start studying the rest of the slices. In order to do that, we will start with the first singular slice $m = m_8 = 1$ below the main slice we have studied. But we will not draw all the bifurcation diagram of it. We will just focus our attention on the part of the bifurcation diagram where the changes occur. We will denote with red labels those parts which remain the same as in the previous slice, and denote with black labels the new parts that appear.

In this way, in slice $m = m_8 = 1$ the only relevant fact is that the parts $4.5L_1$, $5.6L_1$ and $4.6L_1$ coalesce at P_1 (in fact, this is simply the triple intersection of surfaces $\mathcal{S}_4$, $\mathcal{S}_5$ and $\mathcal{S}_6$), thus parts V_{17}, $5S_2$, $6S_6$ and $4S_2$ disappear. In fact, also surface $\mathcal{S}_3$ intersects there and the part V_{11} altogether with its borders coalesces at P_1. Moreover, the singularity of surface $\mathcal{S}_4$ at $4.4L1$ also coalesces at the same point P_1 and this forces the collapse of other parts of the diagram. So, only one new part P_1 appears in this slice which corresponds to a single point in the parameter space (see Figure 5).

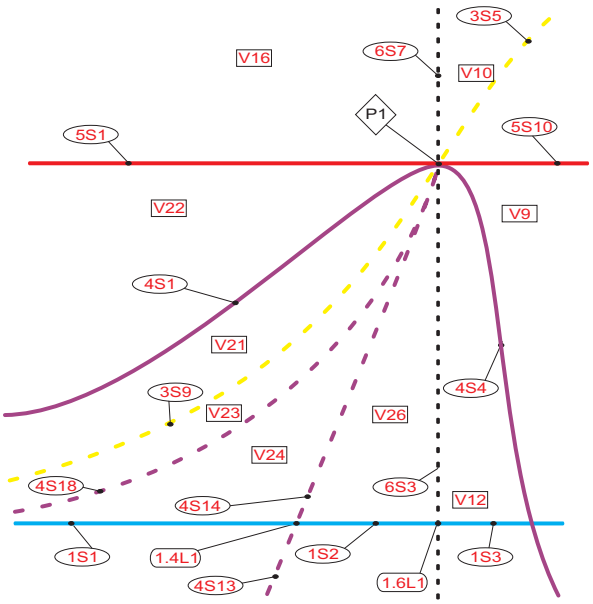

FIGURE 5. Bifurcation diagram for $m = 1$.

The next slice is $m = m_7 = 2/3$ and it is generic. The intersection of several bifurcation surfaces produced in P_1 splits again. We see the born of parts V_{44}, V_{45} and V_{46}, altogether with all their borders. This has been a higher level bifurcation since it has been an intersection of four surfaces, when generically we have intersections of three surfaces in singular slices (see Figure 6).

The next (singular) slice is $m = m_6 = 1/2$. Here part V_{26} and all its borders coalesce at P_2. This is the most typical bifurcation that can be found in these kind of diagrams: Three surfaces intersect at one point, and one "triangular" part disappears with all its borders (three "curves" and three "points") and reappears later at the other side of the bifurcations with new names (see Figure 7). In fact, for this slice, another bifurcation happens: the parts $4S_{12}$ and $3S_{12}$ (which border part V_{41} on the right part of the diagram) that we can see in Figure 6, coincide at infinity. So, we do not notice any difference yet, but after the singular slice we will see some new parts appearing there.

The next slice is $m = m_5 = 2/5$ and it is generic. We draw it larger since we have to reflect changes in different parts of the diagram. A new part V_{47} (altogether with its borders) appears from P_2. Moreover, new unbounded part V_{48} appears together with two 2-dimensional parts $3S_{15}$ and $4S_{25}$ plus a 1-dimensional part $3.4L_4$ (see Figure 8).

The next (singular) slice is $m = m_4 = 1/3$. Here part V_{41} and all its borders coalesce at P_3 in a generic triple intersection of surfaces (see Figure 9).

The next slice is $m = m_3 = 2/7$ and it is generic. The "triangle" around V_{41} reappears as V_{49} and its new borders (see Figure 10).

The next (singular) slice is $m = m_2 = 1/4$. Here part V_{12} and all its borders coalesce at P_4 in a generic triple intersection of surfaces (see Figure 11).

The next slice is $m = m_1 = 1/8$ and it is generic. The "triangle" around V_{12} reappears as V_{50} and its new borders (see Figure 10).

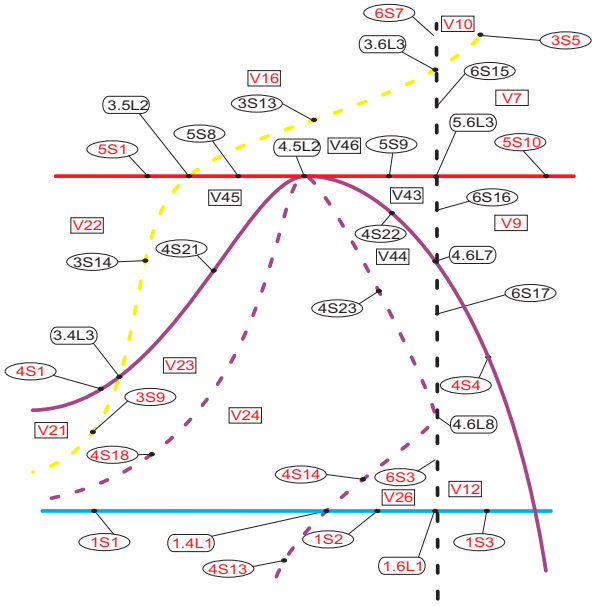

FIGURE 6. Bifurcation diagram for $m = 2/3$.

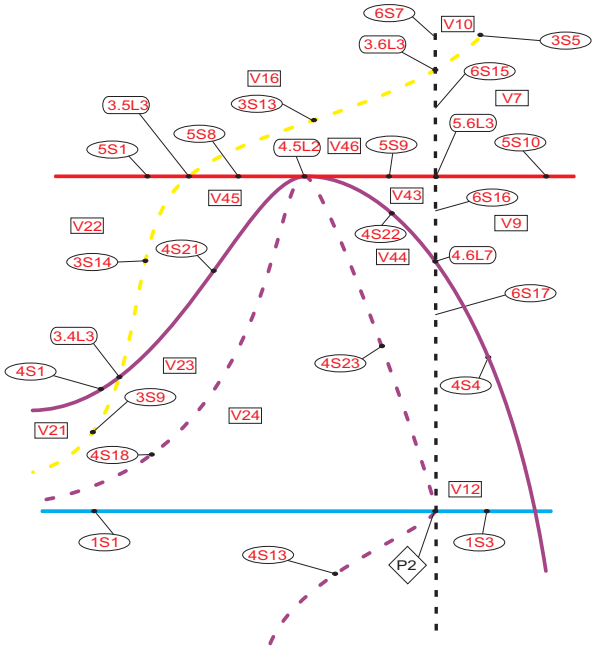

FIGURE 7. Bifurcation diagram for $m = 1/2$.

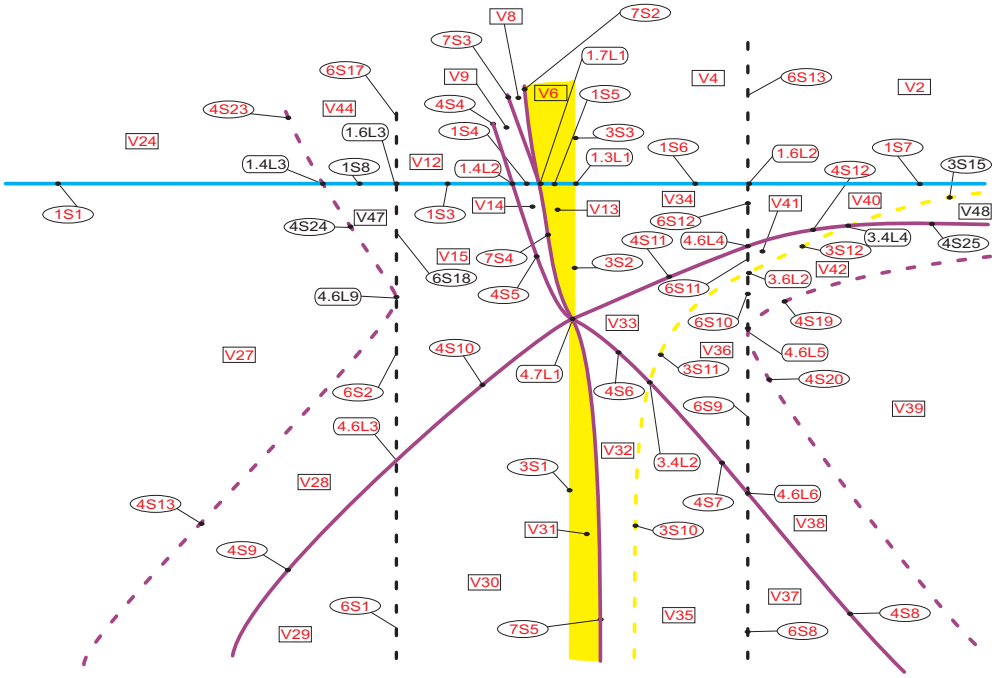

FIGURE 8. Bifurcation diagram for $m = 2/5$.

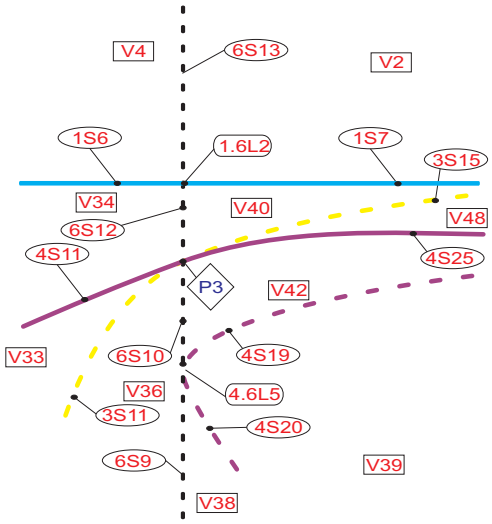

FIGURE 9. Bifurcation diagram for $m = 1/3$.

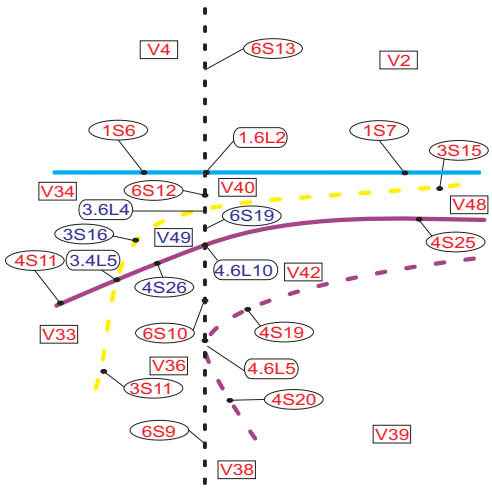

FIGURE 10. Bifurcation diagram for $m = 2/7$.

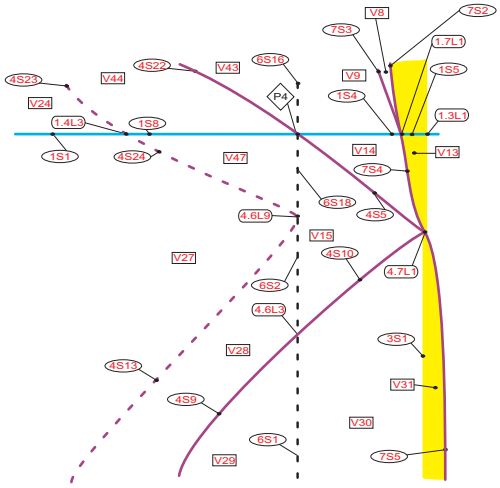

FIGURE 11. Bifurcation diagram for $m = 1/4$.

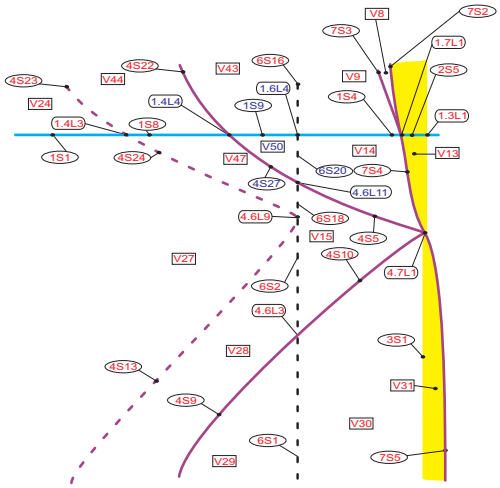

FIGURE 12. Bifurcation diagram for $m = 1/8$.

Finally we arrive to the bottom-most slice $m = m_0 = 0$ and we will plot it, not as an affine plane but as compactified disc including as its border the case $m = n = 0$. In this slice, all the parts are new and denoted with black labels; the generic 2-dimensional parts are really 2-dimensional parts of the bifurcation diagram, as well as the same with other lower dimension parts. Notice that for this slice (and also for the cases $m = n = 0$) there is a vertical symmetry $f \to -f$. Notice also that in contraposition with what would have happened if the compactified parameter space would have been the projective space, we do not have an identification of the opposite equator points, but an identification of points from the upper half cercle to the bottom one. That is, The point P_{18} corresponds to P_{16} and the parts $8.9L_1$ and $8.9L_2$ correspond to $8.9L_4$ and $8.9L_3$ respectively (see Figure 13).

It is important at this point to check, region by region, that the 2-dimensional parts in this slice are the borders of one 3-dimensional part from the slice $m = m_1 = 1/8$, and that if some 2-dimensional part in $m = m_1 = 1/8$ has no continuity in $m = m_0 = 0$, it is because it has collapsed into one of the 1-dimensional parts, or even 0-dimensional parts of slice $m = m_0$. Every phase portrait in slice $m = m_1$ must be explained as the perturbation of a phase portrait in $m = m_0$. We have done this work, region by region, but here we are going to describe only some few examples. Part V_{39} which is present in all slices (see Figures 7 or 8) has $8S_8$ as its bottom border. Part V_{15} which is also present in all slices and we can see it in last Figure 12, collapses at point P_{10}. All the parts that we have seen between surfaces $\mathcal{S}_1$ and $\mathcal{S}_5$ (which appear

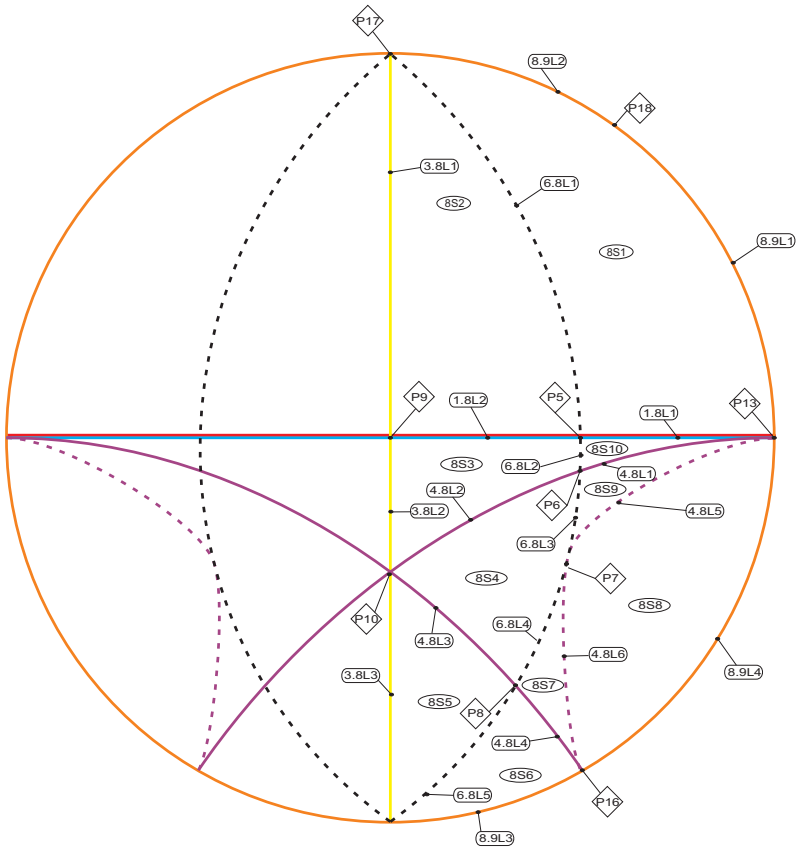

FIGURE 13. Bifurcation diagram for $m = 0$.

as parallel lines in every slice) collapse in different segments or points of the axis $\ell = 0$. It is this coherence in continuity between the parts on slice $m = m_0$ and parts on $m = m_1$ along with the continuity in their associated phase portraits which supports the argument that we are not leaving unstudied any non algebraic singular slice between they both.

We have moved from initial slice $m = m_9 = 3/2$ down up to $m = m_0$, but now we must move up.

So we take the next slice $m = m_{10} = 2$ and we see there that the parts $5.7L_2$ and $3.5L_2$ from Figure 4 coalesce at P_{19}. In this case, the only part that has collapsed is $5S_{10}$ (see Figure 14).

The rest of slices simply follow the movement of the end point of surface $\mathcal{S}_7$ along surface $\mathcal{S}_5$. For $m = m_{11} = 3$ it ends at $5.7L_3$ splitting part $5S_3$ into a new $5S_{11}$ (see Figure 15). For $m = m_{12} = 4$ it ends at P_{20} (see Figure 16) and for $m = m_{13} = 5$ it ends at $5.7L_4$ splitting part $5S_2$ into a new $5S_{12}$ (see Figure 17).

There is no other algebraic singular slice above $m = m_{13}$ so we move to the top cover as $m \to \infty$ which can be seen as system (1) when $n = 0$ (and thus we may take $m = 1$ as explained before). We again draw this slice as a compactified disc, including the border as the equator of the parameter space. In this casse, we have a symmetry $l \to -l$ which coincides with the symmetry we have at the border of the disc (see Figure 18).

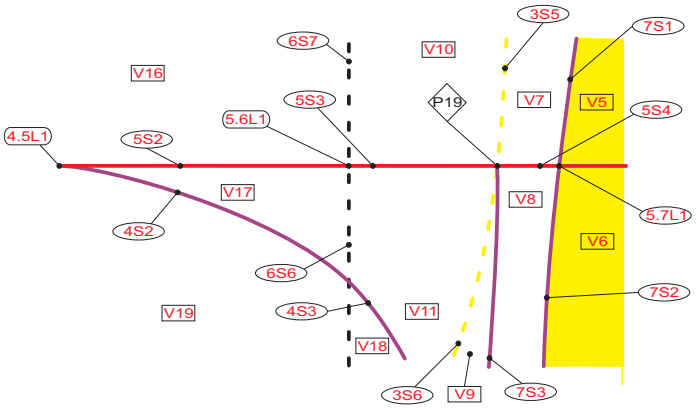

FIGURE 14. Bifurcation diagram for $m = 2$.

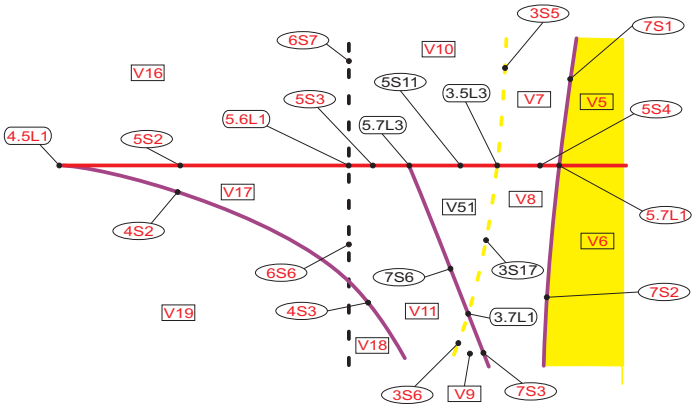

FIGURE 15. Bifurcation diagram for $m = 3$.

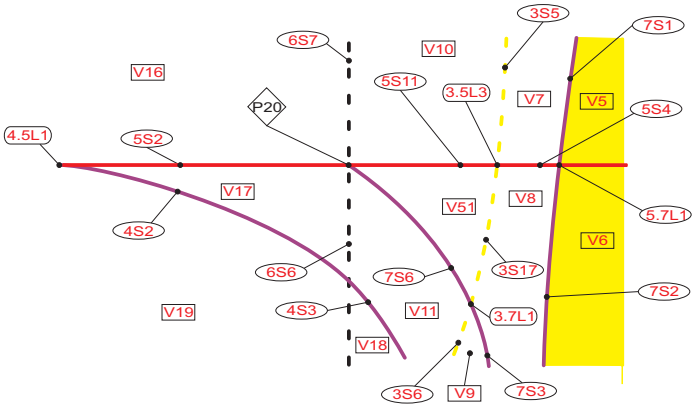

FIGURE 16. Bifurcation diagram for $m = 4$.

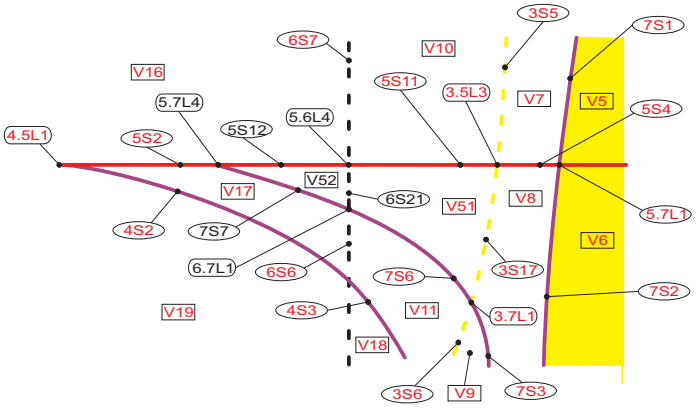

FIGURE 17. Bifurcation diagram for $m = 5$.

As we have done for slice $m = m_0$ we have checked that every part in this slice is the border of one region in slice $m = m_{14}$ or suposses the collapse of several of them giving coherence to the whole bifurcation diagram, and corroborating that no extra non-algebraic singular slice is needed to complete the study.

Remark 2. *Even this may seem quite a complicate bifurcation diagram if this is the first time that the reader sees in a 4-dimensional parameter space (reduced to 3 dimensions with the technique already explained), in fact it is quite simple compared with other works of the same type as* [18] *where more than 50 slices were needed, more than 600 parts were produced, and more than 200 different phase portraits were found. Moreover, it is worth to notice also that in all the singular slices that have appeared here, all the intersections of surfaces involved at most two solid curves, while the other where dashed ones. This has a very important consequence and this is that every slice from $m = m_1$ to $m = m_{14}$, whether if they are generic or singular, contain always all the different topological phase portraits. No set of parts corresponding to a same phase portrait, completely collapses as we move from one slice to another. The slices $m = m_0$ and $m = m_{14}$ contain different phase portraits that had already been found in previous works, but the goal of this paper was precisely to find the rest of cases. So, it seems as if we had done too much extra work by finding the complete bifurcation diagram while only any slice of it would have sufficed to do it, but one cannot be sure of that fact until one has completed the whole*

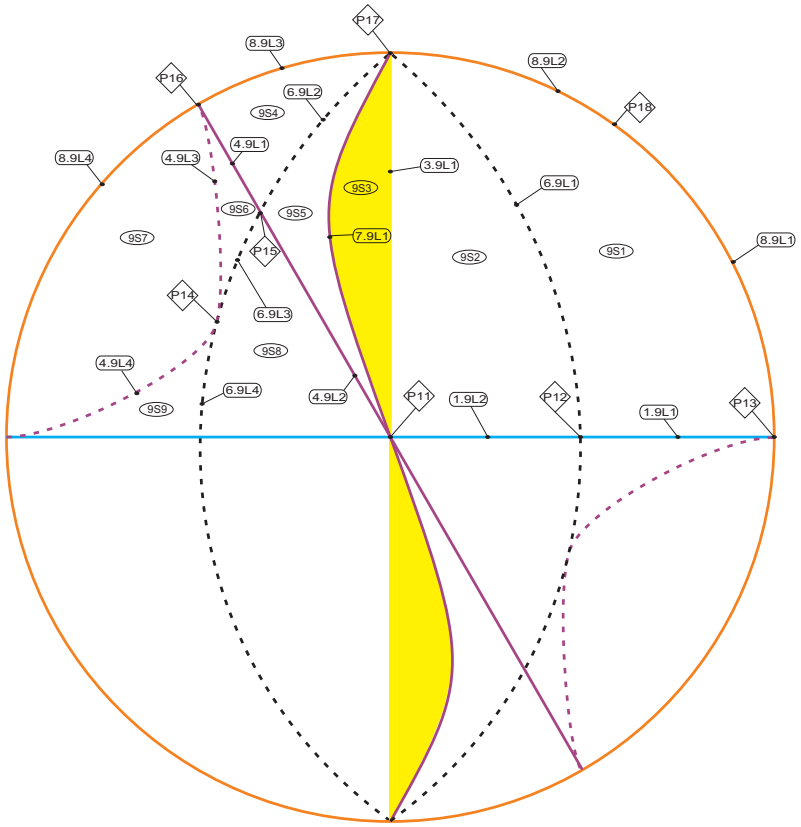

FIGURE 18. Bifurcation diagram for $m = \infty$.

study. Moreover, some geometrical features as having two invariant straight lines in $4.4L_1$ *or coincidences of geometrical features as having an invariant parabola with a node with a double eigenvalue as in* P_{20} *are only available after the complete study since these phenomena appear only in some slices and not in others. This proves that it was not possible a further reduction os parameters from normal form* (1) *to one parameter less.*

4.1. **Compararition with the Ph. D. Thesis of B. Coll.**

In [19] (1987) B. Coll made the closest attempt for the complete study of this family. And he was very close to obtain the full set of different phase portraits that we found here. He missed only two, concretely $4.5L_1$ and $4.7L_1$. Coll tried to study this 4 dimensional parameter space by choosing some wisely selected straight lines on it which covered all the possible cases. Such attempt in a more complicated family would have been a complete failure since just lines in a 4 dimensional space (or even a 3 dimensional one) would be just a splinter of the whole set. But thanks to Remark 2, a good election of lines in a two dimensional space, has more possibilities to be close to completeness. With two more wisely elected lines, he would have achieved it. Anyway, this could not have been accepted as a proof since the complete study was needed.

4.2. **Possible islands in the parameter space.**

In every paper of this kind, this is a compulsory subsection that we must add. We have done our bifurcation diagram for systems (1) and our main theorem claims that there are 49

topologically different phase portrait in it. But this "there exists" must not be read as "there exist exactly" but as "there exists at least". The reason is that there may be non algebraic bifurcations, mainly related with double limit cycles or separatrix connections which could escape to this study. In this family, we cannot have double limit cycles since Rychov [40] already proved the uniqueness and hyperbolicity. But more separatrix connections could exist. However, since we have proved the completeness and coherence of the bifurcation diagram as it is given here, we have proved that no other bifurcation is needed in order to describe it. So, if any other separatrix connection were possible, this should have to take place on the border of a bubble and inside it, we could maybe have a different phase portrait. Since such bubbles, in case they exists, could have any small size, it is not worth trying to find them by a numerical search. It would already be worthless in a 2-dimensional space, even much more in a 4-dimensional one. This is why we have called them "islands". It is also worth to mention that in none of the previous families studied up to now with this technique, such an island has ever been proved to exist.

5. Completion of the proof of Theorem 1

5.1. **Topological Invariants.**

We have split the bifurcation diagram in 261 different parts of different dimensions from 0 to 3. We already know by the type of bifurcations we have found, that some of them only produce geometrical changes that do not affect to the topology of the phase portrait, the most common of them being changes from node to focus, invariant straight lines which are not connection of separatrices and weak saddles. But even reducing all these facts, it is still possible that two separated parts of the bifurcation diagram may have topologically equivalent phase portraits, which initially have been drawn in such a way that it is not easy to compare them to decide if they are the same or not. Of course, one can do a comparison two by two of all the phase portraits and decide if they are the same or not, but apart from the lack of rigor of such a proof, it is easy to make mistakes there. Since similar works have had the duty of distinguishing among hundreds of phase portraits, we better use the same technique as them.

We will create a set of topological invariants such that they may be assigned to each part of the bifurcation diagram. Let S be a quadratic system of Class I.

Definition 1. *Let $p_1, \ldots, p_n$ (with $n \leq 4$) be the finite singularities of S and assume that each one of them receives (or sends) respectively $s(p_1), \ldots, s(p_n)$ separatrices. We define $\mathcal{I}_1(S)$ as the chain of $s(p_1), \ldots, s(p_n)$ such that it produces the biggest possible natural number. If a separatrix arrives to (or departs from) a limit cycle, we will consider it as arriving to the interior focus. For example, if we have two finite singularities, one is a saddle which has 4 separatrices and another is an antisaddle receiving one separatrix, then $\mathcal{I}_1 = 41$.*

Definition 2. *Let $p_1, \ldots, p_n$ (with $n \leq 6$) the infinite singularities of S and each one of them receives (or sends) $s(p_1), \ldots, s(p_n)$ separatrices without taking into consideration the ones which lay on the intinity. We define $\mathcal{I}_2(S)$ as the chain of $s(p_1), \ldots, s(p_n)$ ordered such that starting from whichever point, and moving either clockwise or counter-clocwise sense, the integer produced is the biggest possible. For example, phase portrait V_2 has six singularities at infinity which starting at the point $[0:0]$ of local chart U_2 and moving clockwise sense has $\mathcal{I}_2(S) = 411010$. If we had moved the other sense, the number would have been lower. Since a phase portrait is equivalent to any rotation or symmetry of itself, in this way we are sure to assign the same number to any equivalent phase portrait.*

Definition 3. *We define $I_3(S)$ as the number of limit cycles of S.*

Definition 4. *We define $I_4(S)$ as 1 if S has a center or 0 if not.*

Definition 5. *We define $I_5(S)$ as the maximum number of separatrices received (or sent) by an elemental singularity at infinity.*

This last invariant is needed to distinguish two phase portraits which seem very similar but they are not equivalent. In $5S_6$ an infinite node receives three separatrices, and there is a nilpotent saddle-node which has one separatrix, and receives another from a finite saddle. However in $5S_4$ the elemental infinite node node only receives 2 separatrices, and the infinite nilpotent saddle-node, apart from its own separatrix, receives two separatrices from the finite saddle.

Theorem 2. *The invariant $\mathcal{I} = (\mathcal{I}_1, \mathcal{I}_2, \mathcal{I}_3, \mathcal{I}_4, \mathcal{I}_5)$ makes a partition in the set of phase portraits of quadratic systems of class I (see Table 1). Moreover, for each value of $\mathcal{I}$ there is a unique phase portrait from Figure 1, i.e., $\mathcal{I}(S) = \mathcal{I}(S')$ if and only if S is topologically equivalent to S'.*

In Table 1, if the name of the phase portrait is given inside square brackets, it means the phase portrait has a limit cycle. If it is given inside one set of brackets {}, it means that it has one graphic. If it is given inside two set of brackets {{}}, it means that it has two graphics (in this sense, we consider the infinite set of graphics formed by an elliptic sector are just one including its external border).

$$
I_1 = \left\{ \begin{array}{l}
0 \;\&\; I_2 = \left\{ \begin{array}{l} 0\ \{P_{13}\}, \\ 1010\ \{\{P_{11}\}\}, \\ 2000\ \{P_9\}, \\ 111010\ \{1.7L_1\}, \end{array} \right. \\
1 \;\&\; I_2 = \left\{ \begin{array}{l} 1110\ \{1.9L_1\}, \\ 2100\ (1.8L_1), \\ 110100\ (1.4L_2), \\ 111110\ (1S_4), \\ 211010\ \&\; I_3 = \left\{ \begin{array}{l} 0\ (1S_6), \\ 1\ [1S_5], \end{array} \right. \end{array} \right. \\
2 \;\&\; I_2 = 110110\ (1S_1), \\
40 \;\&\; I_2 = \left\{ \begin{array}{l} 11 \;\&\; I_4 = \left\{ \begin{array}{l} 0\ \{7S_1\}, \\ 1\ \{3.8L_1\}, \end{array} \right. \\ 2101\ \{\{7.9L_1\}\}, \\ 2200\ \{5.7L_1\}, \\ 110110\ \{4.7L_1\}, \\ 111111\ \&\; I_4 = \left\{ \begin{array}{l} 0\ \{7S_4\}, \\ 1\ \{3.8L_2\}, \end{array} \right. \\ 220110\ \&\; I_4 = \left\{ \begin{array}{l} 0\ \{7S_5\}, \\ 1\ \{3.8L_3\}, \end{array} \right. \\ 311010\ \{7S_2\}, \end{array} \right. \\
41 \;\&\; I_2 = \left\{ \begin{array}{l} 21 \;\&\; I_3 = \left\{ \begin{array}{l} 0\ (V_1), \\ 1\ [V_5], \end{array} \right. \\ 1110\ \{4.9L_1\}, \\ 2100\ (5.7L_2), \\ 2101\ \{9S_6\}, \\ 2210\ \{9S_4\}, \\ 3101\ \&\; I_3 = \left\{ \begin{array}{l} 0\ \{9S_1\}, \\ 1\ \{[9S_3]\}, \end{array} \right. \\ 3200\ \&\; I_3 = \left\{ \begin{array}{l} 0\ \&\; I_5 = \left\{ \begin{array}{l} 2\ (5S_4), \\ 3\ (5S_6), \end{array} \right. \\ 1\ [5S_5], \end{array} \right. \\ 111110\ (4S_5), \\ 210110\ (4S_6), \\ 211010\ (7S_3), \\ 211111\ \&\; I_3 = \left\{ \begin{array}{l} 0\ (V_{14}), \\ 1\ [V_{13}], \end{array} \right. \\ 320110\ \&\; I_3 = \left\{ \begin{array}{l} 0\ (V_{29}), \\ 1\ [V_{31}], \end{array} \right. \\ 321010\ (V_8), \\ 411010\ \&\; I_3 = \left\{ \begin{array}{l} 0\ (V_2), \\ 1\ [V_6], \end{array} \right. \end{array} \right. \\
42 \;\&\; I_2 = \left\{ \begin{array}{l} 2101\ (5S_1), \\ 111010\ (4S_1), \\ 211110\ \&\; I_5 = \left\{ \begin{array}{l} 1\ (V_{15}), \\ 2\ (V_9), \end{array} \right. \end{array} \right. \\
43 \;\&\; I_2 = \left\{ \begin{array}{l} 2120\ (4.5L_1), \\ 111110\ (V_{12}), \end{array} \right.
\end{array} \right.
$$

TABLE 1. Classification of the phase portraits according to the invariants of Theorem 2.

Proof. This theorem comes from a simple application of the invariants to all the phase portraits from all the regions of the bifurcation diagram. If a region does not appear in this list is because it has exactly the same invariants as one already displayed, and then, it has been checked that the phase portraits are really the same. In the next subsection we give the correlation among all the parts that do not appear here (and thus neither in Figure 1) and the ones we have selected of representatives of their classes (the most generic one with lower index). Note that a phase portrait from one part of the diagram may have a focus while from another part, it may be exactly the same, except it has a node. In Figure 1 they are drawn indistinctly as focus or nodes depending of the representative chosen. □

5.2. **Table of topological equivalences.**

In this section we will give Table 2 where we link the representative of every phase portrait given in Figure 1 with all the different regions in which the parameter space has been divided. Two phase portraits from different regions may be topologically equivalent for different reasons. The most common ones that we will see here are that a phase portrait has a focus and another a node, or one has a weak singularity (focus or saddle) while the other has a strong singularity of the same type, or a system has an invariant straight line which does not conform a separatrix connection and thus, it may be equivalent to another phase portrait without such geometrical property. But there are other different reasons and in other classifications may also appear new ones (multiple singularities with equivalent phase portrait, or simply the same phase portrait appears in a region far from the first).

We will group them along several columns putting on the left column the representative region, and in the same row, the equivalent portraits. Moreover, in different sub rows, we will group the equivalent regions according the dimension of the part they have. That is, the regions having the same dimension as the representative phase portrait will be in the exactly same line, and below we will have other regions of lower dimension. For the representative regions, we have always taken one of the biggest possible dimension and with the lowest cardinal.

If several consecutive named regions belong to the same block, we have joined them as in V_{19-21} in order to reduce the width of the table.

Proof of Theorem 1. The union of Sections 4 and 5 conforms the proof of the theorem since we have found a complete and coherent partition of the parameter space, and have extracted from it the set of topologically different phase portraits. □

Declarations

Funding. J.C. Artés is supported by Agencia Estatal de Investigación grant PID2019-104658GB-I00, the H2020 European Research Council grant MSCA-RISE-2017-777911 and the AGAUR (Generalitat de Catalunya) grant 2021-SGR 00113. H. Chen is supported by the National Natural Science Foundation of China (Nos. 12322109 and 12171485), and by Science and Technology Innovation Program of Hunan Province (No. 2023RC3040). M. Jia is supported by the China Postdoctoral Science Foundation (No. 2023M743969) and Postdoctoral Fellowship Program of CPSF (No. GZC20233195).

Data Availibility. No new data or materials have been used in the preparation of this paper.

Conflict of interest. The authors declare that they do not have any interests of a financial or personal nature.

Ethical Approval. Not applicable.

Competing interests. This manuscript has not been published and is not under consideration for publication elsewhere.

Main phase portrait	Focus - node	Weak focus of order 1	Weak saddle	Invariant straight line	Other reasons
V_1	V_3 $6S_{14}$, $6S_7$, $6S_{15}$ $6.8L_1$	$3S_4$	$3S_5$, $3S_{13}$ $3.6L_3$		V_7, V_{10}, V_{16}, V_{46} $8S_{1-2}$ $8.9L_{1-4}$ P_{16}, P_{18}
V_2	V_4 $6S_{13}$	$3S_3$			
V_5					
V_6					
V_8	 $6S_{21}$		 $3S_{17}$		V_{51-52}
V_9	V_{17},V_{43} $6S_6$, $6S_{16}$		 $3S_6$, $3S_{14}$		V_{11}, V_{22}, V_{45}
V_{12}	V_{19-21}, V_{23-26}, V_{44} $6S_{3-5}$, $6S_{17}$ $3.6L_1$		$3S_{7-9}$	$4S_{14-18}$, $4S_{23}$ $4.4L_1$, $4.6L_2$, $4.6L_8$	V_{18}
V_{13}					
V_{14}	V_{50} $6S_{12}$, $6S_{19}$, $6S_{20}$ $6.8L_2$	$3S_2$	$3S_{15}$ $3S_{16}$ $3.6L_4$		V_{34}, V_{40}, V_{48-49} $8S_3$, $8S_{10}$
V_{15}	V_{27}, V_{28}, V_{47} $6S_2$, $6S_{9-11}$, $6S_{18}$ $6.8L_3$, $6.8L_4$		$3S_{11}$, $3S_{12}$ $3.6L_2$	$4S_{13}$, $4S_{19-20}$, $4S_{24}$ $4.6L_5$, $4.6L_9$, $4.8L_{5-6}$ P_7	V_{33}, V_{36}, V_{38-39}, V_{41-42} $8S_4$, $8S_{7-9}$
V_{29}	V_{30} $6S_1$, $6S_8$ $6.8L_5$	$3S_1$	$3S_{10}$		V_{32}, V_{35}, V_{37} $8S_5$, $8S_6$
V_{31}					

TABLE 2.

Main phase portrait	Focus - node	Weak focus of order 1	Weak saddle	Invariant straight line	Other reasons
$1S_1$	$1S_3$ $1.6L_1$, $1.6L_3$			$1.4L_1$, $1.4L_3$ P_2	$1S_2$, $1S_8$
$1S_4$	$1S_9$ $1.6L_4$				
$1S_5$					
$1S_6$	$1S_7$ $1.6L_2$	$1.3L_1$			
$4S_1$	 $4.6L_1$, $4.6L_7$		$3.4L_1$, $3.4L_3$		$4S_{2-4}$, $4S_{21-22}$
$4S_5$	$4S_{27}$ $4.6L_4$, $4.6L_{10-11}$ P_6		$3.4L_{4-5}$ P_3		$4S_{11-12}$, $4S_{25-26}$ $4.8L_{1-2}$
$4S_6$	$4S_8$ $4.6L_3$, $4.6L_6$ P_8		$3.4L_2$		$4S_7$, $4S_9$, $4S_{10}$ $4.8L_{3-4}$
$5S_1$	 $5.6L_1$		$3.5L_2$		$5S_{2-3}$, $5S_8$, $5S_{10}$
$5S_4$	$5S_9$ $5.6L_{3-4}$		$3.5L_3$	$5S_{11-12}$	
$5S_5$					
$5S_6$	$5S_7$ $5.6L_2$	$3.5L_1$			
$7S_1$					
$7S_2$					
$7S_3$	$7S_5$		 $3.7L_1$		
$7S_4$					
$7S_5$					
$9S_1$	$9S_2$ $6.9L_1$	$3.9L_1$			
$9S_3$					
$9S_4$	$9S_5$ $6.9L_2$				

TABLE 3. Continuation of Table 2.

Main phase portrait	Focus - node	Weak focus of order 1	Weak saddle	Invariant straight line	Other reasons
$9S_6$	$9S_8$ $6.9L_{3-4}$			$4.9L_{3-4}$ P_{14}	$9S_7$, $9S_9$
$1.4L_2$	$1.4L_4$ P_4				
$1.7L_1$					
$1.8L_1$	$1.8L_2$ P_5				
$1.9L_1$	$1.9L_2$ P_{12}				
$3.8L_1$					P_{17}
$3.8L_2$					
$3.8L_3$					
$4.5L_1$	P_1				$4.5L_2$
$4.7L_1$					P_{10}
$4.9L_1$	$4.9L_2$ P_{15}				
$5.7L_1$					
$5.7L_2$				$5.7L_{3-4}$ P_{19-20}	
$7.9L_1$					
P_9					
P_{11}					
P_{13}					

TABLE 4. Continuation of Table 2.

References

[1] J.C. Artés, F. Dumortier, J. Llibre, Limit cycles near hyperbolas in quadratic systems, *J. Differential Equations*, **246**(2009) 235-260.

[2] J.C. Artés, R.E. Kooij, J. Llibre, Structurally stable quadratic vector fields, *Mem. Am. Math. Soc.*, **134**(1998) 1-108.

[3] J.C. Artés, J. Llibre, J.C. Medrado, Nonexistence of limit cycles for a class of structurally stable quadratic vector fields, *Discrete Contin. Dyn. Syst.*, **17**(2007) 259-271.

[4] J.C. Artés, J. Llibre, A.C. Rezende, *Structurally Unstable Quadratic Vector Fields of Codimension One*, Birkhäuser, Cham, 2018.

[5] J.C. Artés, J. Llibre, A. C. Rezende, D. Schlomiuk, N. Vulpe, Global configurations of singularities for quadratic differential systems with exactly two finite singularities of total multiplicity four, *Electron. J. Qual. Theory Differ. Equ.*, **2014**(2014) 60-1-43.

[6] J.C. Artés, J. Llibre, D. Schlomiuk, The geometry of quadratic differential systems with a weak focus of second order, *Internat. J. Bifur. Chaos*, **16**(2006) 3127-3194.

[7] J.C. Artés, J. Llibre, D. Schlomiuk, The geometry of quadratic polynomial differential systems with a weak focus and an invariant straight line, *Internat. J. Bifur. Chaos*, **20**(2010) 3627-3662.

[8] J.C. Artés, J. Llibre, D. Schlomiuk, N. Vulpe, Configurations of singularities for quadratic differential systems with total finite multiplicity lower than 2, *Bul. Acad. Ştiinţe Repub. Mold. Mat.*, **71**(2013) 72-124.

[9] J.C. Artés, J. Llibre, D. Schlomiuk, N. Vulpe, Geometric configurations of singularities for quadratic differential systems with three distinct real simple finite singularities, *J. Fixed Point Theory Appl.*, **14**(2013) 555-618.

[10] J.C. Artés, J. Llibre, D. Schlomiuk, N. Vulpe, Geometric configurations of singularities for quadratic differential systems with total finite multiplicity $m_f = 2$, *Electron. J. Differ. Equ.*, **2014**(2014) 159-1-79.

[11] J.C. Artés, J. Llibre, D. Schlomiuk, N. Vulpe, Global configurations of singularities for quadratic differential systems with total finite multiplicity three and at most two real singularities, *Qual. Theory Dyn. Syst.*, **13**(2014) 305-351.

[12] J.C. Artés, J. Llibre, D. Schlomiuk, N. Vulpe, Global configurations of singularities for quadratic differential systems with exactly three finite singularities of total multiplicity four, *Electron. J. Qual. Theory Differ. Equ.*, **2015**(2015) 49-60.

[13] J.C. Artés, J. Llibre, D. Schlomiuk, N. Vulpe, From topological to geometric equivalence in the classification of singularities at infinity for quadratic vector fields, *Rocky Mountain J. Math.*, **45**(2015) 29-113.

[14] J.C. Artés, J. Llibre, D. Schlomiuk and N. Vulpe, *Geometric configurations of singularities of planar polynomial differential systems - A global classification in the quadratic case*. Birkhäuser/Springer, Cham, xii+699 pp. ISBN: 978-3-030-50569-1; 978-3-030-50570-7, 2021.

[15] J.C. Artés, A.C. Rezende, R. Oliveira, Global phase portraits of quadratic polynomial differential systems with a semi-elemental triple node, *Internat. J. Bifur. Chaos*, **23**(2013) 1350140–1-21.

[16] J.C. Artés, A.C. Rezende, R. Oliveira, The geometry of quadratic polynomial differential systems with a finite and an infinite saddle-node (A,B), *Internat. J. Bifur. Chaos*, **24**(2014) 1450044–1-30.

[17] J.C. Artés, A.C. Rezende, R.D.S. Oliveira, The geometry of quadratic polynomial differential systems with a finite and an infinite saddle-node (C), *Internat. J. Bifur. Chaos*, **25**(2015) 1530009–1-111.

[18] J.C. Artés, M.C. Mota and A.C. Rezende *Quadratic differential systems with a finite saddle-node and an infinite saddle-node (1, 1)SN - (B)* Int. Journal of Bifurcation and chaos **31**(2021), 2130026–110pp

[19] B. Coll, Estudi qualitatiu d'algunes classes de camps vectorials al pla., *Ph. D. Thesis Universitat Autnoma de Barcelona*, (1987).

[20] W.A. Coppel, A survey of quadratic systems, *J. Differential Equations*, **2**(1966) 293-304.

[21] W.A. Coppel, Some quadratic systems with at most one limit cycle, *Dynamics Reported*, **2**(1989) 61-88.

[22] W.A. Coppel, A new class of quadratic systems, *J. Differential Equations*, **92**(1991) 360-372.

[23] F. Dumortier, J. Llibre, J.C. Artés, *Qualitative Theory of Planar Differential Systems*, Springer-Verlag, New York, 2006.

[24] A. Ferragut, J.D. Garcia-Saldana, C. Valls, Phase portraits of Abel quadratic differential systems of second kind with symmetries. *Dynamical Syst.*, **34**(2019), 301-333.

[25] A. Ferragut, C. Valls, Phase portraits of Abel quadratic differential systems of the second kind, *Dynamical Syst.*, **33**(2018), 581-601.

[26] A. Gasull, H. Giacomini, S. Pérez-González, J. Torregrosa, A proof of Perko's conjectures for the Bogdanov-Takens system, *J. Differential Equations*, **255**(2013) 2655-2671.

[27] M.R.A. Gouveia, J. Llibre, L.A. Roberto, Phase portraits of the quadratic polynomial Liénard differential systems, *Proc. Roy. Soc. Edinburgh*, **151**(2021) 202-216.

[28] D. Hilbert. Mathematische probleme. In Nachr. Ges. Wiss., editor, *Second Internat. Congress Math. Paris, 1900*, pages 253–297. Göttingen Math.–Phys. Kl., 1900.

[29] D. Hilbert. Mathematical problems. *Bull. Amer. Math. Soc.*, **8**(1902) 437–479.

[30] Y. Ilyashenko, Centennial history of Hilbert's 16th problem, *Bull. Am. Math. Soc.*, **39**(2002) 301-354.

[31] M. Jia, H. Chen, H. Chen, Bifurcation diagram and global phase portraits of a family of quadratic vector fields in Class I, *Qual. Theo. Dyn. Syst.*, **19**(2020) 64–1-22.
[32] A. Lins, W. de Melo, C.C. Pugh, On Liénard's equation, *Lecture Notes in Math.*, **597**(1977) 335-357.
[33] C. Li, Z. Zhang, Remarks on 16th weak Hilbert problem for $n = 2$, *Nonlinearity*, **15**(2002) 1975-1992.
[34] J. Li, Hilbert's 16th problem and bifurcations of planar polynomial vector fields, *Internat. J. Bifur. Chaos*, **13**(2003) 47-106.
[35] L.M. Perko, A global analysis of the Bogdanov-Takens system, *SIAM J. Appl. Math.*, **52**(1992) 1172-1192.
[36] J.W. Reyn, Phase portraits of quadratic systems without finite critical points, *Nonlinear Anal.*, **27**(1996) 207-222.
[37] J.W. Reyn, Phase portraits of quadratic systems with finite multiplicity one, *Nonlinear Anal.*, **28**(1997) 755-778.
[38] J.W. Reyn, *Phase Portraits of Planar Quadratic Systems*, Mathematics and Its Applications **583**, Springer, New York, 2007.
[39] J.W. Reyn, R.E. Kooij, Phase portraits of non-degenerate quadratic systems with finite multiplicity two, Mathematics and Its Applications, *Differ. Equ. Dyn. Syst.*, **5**(1997) 355-414.
[40] G.S. Rychkov, A complete investigation of the number of limit cycles of the equation $(b_{10}x + y)dy = \sum_{i+j=1}^{2} a_{ij}x^i y^j dx$, *Diff. Equa.* **6**(1970) 2193-2199. (in Russian)
[41] N. Vulpe, Family of quadratic differential systems with invariant parabolas: a complete classification in the space $\mathbb{R}^{12}$. *Electron. J. Qual. Theory Differ. Equ.*, **22**(2024) 1-68.
[42] Y. Ye, *Theory of Limit Cycles*, Transl. Math. Monogr., Amer. Math. Soc., Providence, RI, 1986.
[43] X. Zhang, Q. Ye, Uniqueness of limit cycles of quadratic system $(\mathrm{III})_{m=0}$, *Chinese Sci. Bull.*, **42**(1997) 628-631.
[44] Z. Zhang, T. Ding, W. Huang, Z. Dong, *Qualitative Theory of Differential Equations*, Transl. Math. Monogr., Amer. Math. Soc., Providence, RI, 1992.
[45] H. Zoladek, Quadratic systems with center and their perburbations, *J. Differential Equations*, **109**(1994) 223-273.

[1] Departament de Matemàtiques, Universitat Autònoma de Barcelona, 08193 Bellaterra, Barcelona, Catalonia, Spain
E-mail address: joancarles.artes@uab.cat(J.C. Artés)
E-mail address: lluc.manel@gmail.com (L.M. Ferrer)

[2] School of Mathematics and Statistics, HNP-LAMA, Central South University, 410083 Changsha, Hunan, P. R. China
E-mail address: chen_hebai@csu.edu.cn(H. Chen)
E-mail address: jiaman9305@163.com(M. Jia, corresponding author)